

SUPPLEMENTARY INFORMATION FOR
A Chemical Route to Activation of Open Metal Sites in the Copper-Based Metal-Organic Framework Materials HKUST-1 and Cu-MOF-2

Hong Ki Kim,[†] Won Seok Yun,[†] Min-Bum Kim,[‡] Jeung Yoon Kim,[†] Youn-Sang Bae,[‡] JaeDong Lee,[†] Nak Cheon Jeong^{*,†}

[†]Department of Emerging Materials Science, DGIST, Daegu 711-873, Korea

[‡]Department of Chemical and Biomolecular Engineering, Yonsei University, Seoul 120-749, Korea

*To whom correspondence should be addressed. E-mail: nc@dgist.ac.kr

Table of contents

Sections	Titles	pages
Section S1.	Materials and Methods	SI-2 – SI-4
Section S2.	Structural View of the Arrangement of the Cages within HKUST-1	SI-5
Section S3.	¹ H-NMR and PXRD Results for Thermally Activated HKUST-1	SI-6
Section S4.	BET Results for Thermally and Chemically Activated HKUST-1 Powder Samples	SI-7
Section S5.	Raman Spectra of MC, EtOH, and H ₂ O Solvents	SI-8
Section S6.	Theoretical Studies for Raman Shift of Cu-Cu vibration in HKUST-1	SI-9 – SI-10
Section S7.	Raman Spectra of Activated HKUST-1 after Exposure to Ambient Atmosphere	SI-11
Section S8.	PXRD Patterns of Pristine and Activated Cu-MOF-2	SI-12
Section S9.	¹ H-NMR, Raman, and BET Results for Room Temperature Evacuation of HKUST-1	SI-13
References		SI-14

Section S1. Materials and Methods

Materials. All reagents were obtained from commercial sources (Sigma Aldrich, Alfa Aesar, or Daejung) and were used without further purification. Copper (II) nitrate [$\text{Cu}(\text{NO}_3)_2 \cdot 3\text{H}_2\text{O}$, 98.0-103%, Aldrich], trimesic acid (1,3,5-benzenetricarboxylic acid, BTC, 95%, Aldrich), ethanol (EtOH, 96%, Daejung), N,N-Dimethylformamide (DMF, 99.8%, Aldrich), and distilled deionized water (DDW) were used for synthesis of HKUST-1 in both the crystalline powder and film forms. 1,4-Benzenedicarboxylic acid (BDC, 98+%, Alfa Aesar) was used with copper (II) nitrate for synthesis of Cu-MOF-2 powder. Methylene chloride (CH_2Cl_2 , MC, 99.5%, Aldrich) was employed as a reagent for chemical activation (CA). Anhydrous methanol (MeOH, 99.8%, Aldrich), anhydrous ethanol (EtOH, 99.5%, Aldrich), and anhydrous acetonitrile (MeCN, 99.8%, Aldrich) were employed for substitution of pre-coordinated water and ethanol in pristine HKUST-1. Sulfuric acid- d_2 (D_2SO_4 , 96-98 wt% in D_2O , 99.5 atomic % in deuterium, Aldrich) was used for dissolving HKUST-1 and Cu-MOF-2 prior to performing ^1H -NMR spectroscopy on the samples. Copper-clad laminate board (RS component code: 159–5773) was used for making printed circuit boards (PCBs), which were used as the substrate for the HKUST-1 film, and ammonium persulfate [$(\text{NH}_4)_2\text{S}_2\text{O}_8$, 98%, Aldrich] was used for oxidizing metallic copper prior to synthesis of the HKUST-1 film. All synthesized MOF powders and films were stored in a moisture-free argon-charged glove box prior to use.

Synthesis of HKUST-1. We synthesized HKUST-1 following the procedure described in a previous report.^{S1} Briefly, $\text{Cu}(\text{NO}_3)_2 \cdot 3\text{H}_2\text{O}$ (0.87 g, 3.6 mmol) was dissolved in 10 mL of DDW in a vial. In a separate vial, BTC (0.22 g, 1.0 mmole) was dissolved in 10 mL of EtOH. The $\text{Cu}(\text{NO}_3)_2$ solution was quickly added into the vial in which the BTC solution was contained. After continuous stirring for 10 min at room temperature, 1 mL of DMF was added to the mixed solution. Then, the vial was sealed with polytetrafluoroethylene (PTFE) tape. The vial was placed in an oven at 80 °C for 20 h to allow the mixture to react. After allowing the product to cool to room temperature, we collected and washed the crystalline solid (pristine HKUST-1) with H_2O and EtOH.

Synthesis of Cu-MOF-2. We also synthesized Cu-MOF-2 following the procedure described in previous reports.^{S2-S4} $\text{Cu}(\text{NO}_3)_2 \cdot 3\text{H}_2\text{O}$ (0.242 g, 1.0 mmol) was dissolved in 10 mL of DMF in a vial. In a separate vial, BDC (0.166 g, 1.0 mmol) was dissolved in 10 mL of DMF. The $\text{Cu}(\text{NO}_3)_2$ solution was quickly added to the BDC solution. After continuous stirring for 10 min at room temperature, the vial was sealed with PTFE tape. Then, the vial was placed in an oven at 110 °C for 48 h to allow the mixture to react. After allowing the vial to cool to room temperature, we collected and washed the crystalline solid (pristine Cu-MOF-2) with fresh DMF.

Synthesis of HKUST-1 film on patterned copper-clad laminate plate. HKUST-1 films were synthesized on patterned copper-clad laminate plate. First, the copper-clad plates were patterned using the routine photolithography method. Then, the metallic copper surface was smoothed using a polisher and alumina powder, and the plate was washed with acetone and ethanol. The washed copper plate was put into 2 wt% $(\text{NH}_4)_2\text{S}_2\text{O}_8$ /DDW solution and then allowed to oxidize for 30 s. After washing with DDW, the plate was placed into a plastic box in which 150 mM BTC solution of mixed H_2O and EtOH solvent were contained. Then, the copper substrate was allowed to react with the BTC at 40 °C for 7 d. Subsequently, the HKUST-1 film that was formed was washed with copious amounts of fresh EtOH. Then, the film was transferred into a moisture-free Ar-charged glove box prior to use.

Thermal activation (TA) of HKUST-1 and Cu-MOF-2. Coordinated solvents in pristine HKUST-1 (H_2O and EtOH) and Cu-MOF-2 (DMF) were removed by TA. For this TA, pristine HKUST-1 powder was placed into a glass vacuum tube. Then, the tube was heated at 150 °C for 12 h under vacuum ($\sim 10^{-3}$

torr). The method for the TA of Cu-MOF-2 powder was the same as the above procedure except for the activation temperature, which was approximately 200 °C. After activation, the tubes were transferred into an Ar-charged glove box prior to use.

Chemical activation (CA) of HKUST-1 and Cu-MOF-2. 0.05 g of pristine HKUST-1 powder were placed into 20 mL of MC. Then, the pre-coordinated H₂O and EtOH were removed for 5 min. This process was repeated 5 times to successfully activate the HKUST-1. The process for the chemical activation of Cu-MOF-2 was same as the above procedure except for the number of repetitions of the procedure (12 times). In the case of the HKUST-1 films, the process was achieved by dipping the films into fresh MC solvent for 5 min. This procedure was also repeated 5 times. The entire chemical activation process was performed in a moisture-free argon-charged glove box.

Exchange of coordinated ligands in HKUST-1. The substitution of pre-coordinated solvent molecules in pristine HKUST-1 (H₂O and EtOH) was performed following the procedure described in a previous report.⁵¹ Briefly, thermally activated HKUST-1 powder samples were placed in vials, and methanol (MeOH) was put into the vial. Then, the activated HKUST-1 was allowed to react with the methanol for 1 h. Subsequently, the MeOH-coordinated HKUST-1 (MeOH-HK) that was formed was collected by filtration and dried under an Ar atmosphere before use. Substitution by ethanol (EtOH) and acetonitrile (MeCN) was achieved using the same procedure. All of the processes were conducted under an inert atmosphere in a moisture-free argon-charged glove box.

Sample preparation for the measurement of Raman and UV-vis absorption spectra. Prior to taking Raman and UV-vis absorption spectra, HKUST-1 or Cu-MOF-2 powder samples were contained in cylindrical quartz cells (Starna, Type 37GS Cylindrical Cells with Quartz to Borofloat graded seal). The preparation was performed in a moisture-free Ar-charged glove box, and the cells were sealed with a glass cork using a grease (Apiezon, H high temperature Vacuum Greases) prior to the measurements.

Sample preparation for the ¹H-NMR measurements. A tiny amount of HKUST-1 or Cu-MOF-2 powder was dissolved in 1 mL of D₂SO₄. Then, the solution was transferred into an NMR tube. This preparation was also conducted in an Ar-charged glove box. Additionally, the tubes were sealed with plastic caps and acrylic Parafilm® prior to being removed from the glove box.

Sample preparation for measurement of moisture sorption. To check moisture sorption of thermally activated HKUST-1 (TA-HK), the powder sample (~100 mg) was spread onto a light, shallow plastic container (4 cm × 4 cm) placed on top of a microbalance, and the initial weight of the powder was quickly measured. Then, the increase in the weight of the powder was continuously monitored at intervals of 10 s, with the powder exposed to the ambient atmosphere (relative humidity of ~30%). The chemically activated HKUST-1 (MC-HK) was also examined using the same procedure.

Instrumentation. DDW was obtained from a water purification system (Merck Millipore, MQ Direct 8). Diffuse reflectance UV-vis spectra of samples were recorded using an Agilent Cary 5000 UV-VIS-NIR spectrophotometer. PXRD patterns were obtained using a PANalytical diffractometer (Empyrean) with a monochromatic nickel-filtered Cu K_α beam. ¹H-NMR spectra were recorded using an AVANCE III HD FT-NMR spectrometer (Bruker, 400 MHz for ¹H). The ¹H chemical shifts were referenced to the residual proton resonance of the solvent. Nitrogen adsorption/desorption isotherms of the samples were obtained at 77 K by using a Tristar 3020 surface area and porosity analyzer (Micromeritics). The increase in the weight caused by moisture sorption was measured using a microbalance (Sartorius, Cubis Micro Complete Balance). Optical microscope images were taken using an S43T microscope (Bimeince). Raman spectra were recorded using a Nicolet Omega XR dispersive Raman spectrometer

(Thermo Scientific). Excitation of the samples was performed by focusing a 1.23-mW 532-nm-wave-length laser beam on a crystal with a 10× magnifying objective lens. The instruments used for the PXRD, ^1H NMR, and Raman analyses are located at the Center for Core Research Facilities (CCRF) in DGIST.

Section S2. Structural View of the Arrangement of the Cages within HKUST-1

HKUST-1 has three types of cages and two types of windows (see Figure S1 below).^{S1} Three-dimensional type 1 and type 2 large cages are alternately interconnected and share large windows (see Figures S1d and S1f). The small cages (type 3) formed at the edges of large cages share small windows with type 2 large cages (see Figures S1e and S1f). The sizes of the windows are presented in Figures S1d and S1e. All of the axial OCSs on the $(\text{Cu}^{\text{II}})_2$ centers face the type 1 large cages such that free ligands (i.e., solvents) can be easily accessed.

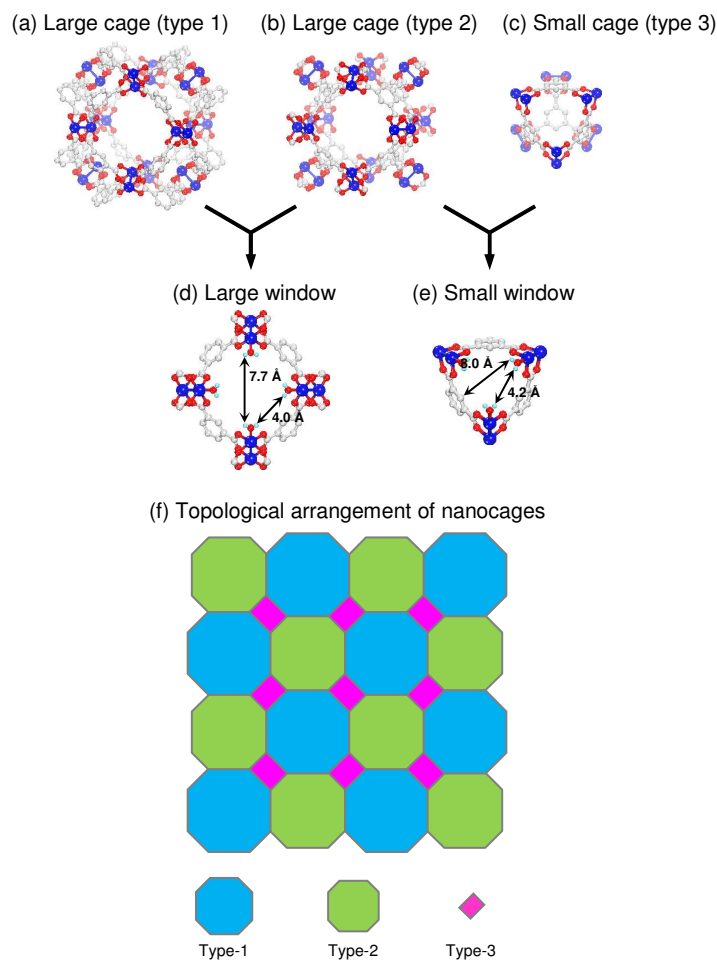


Figure S1. Illustration of cages and windows within HKUST-1 and 2-dimensional representation of the topological arrangement of the cages. Hydrogen atoms bonded to carbon in BTC are omitted for the sake of clarity.

Section S3. ^1H -NMR and PXRD Results for Thermally Activated HKUST-1

^1H -NMR and PXRD tests of a thermally activated HKUST-1 sample were conducted for comparison with the chemical activation results. The NMR data for TA-HK demonstrate that ethanol molecules coordinated to the copper centers in pristine HKUST-1 were removed by the TA (see Figure S2a). The PXRD data indicate that although the coordination bonds were dissociated, the framework of HKUST-1 remained intact (see Figure S2b).

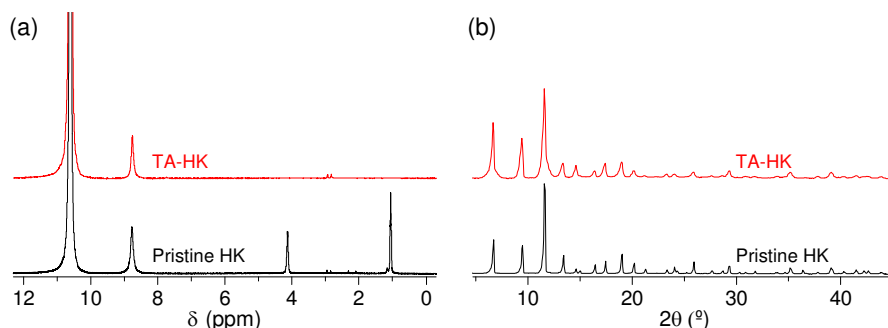


Figure S2. (a) ^1H -NMR spectra and (b) PXRD patterns of pristine-HK and TA-HK powder samples. The TA was performed at 150 $^\circ\text{C}$ for 12 h. The NMR spectra were taken after completely dissolving the powder samples in D_2SO_4 .

Section S4. BET Results for Thermally and Chemically Activated HKUST-1 Powder Samples

We wanted to examine whether chemical activation by MC can be achieved at room temperature and whether the framework of the MOF is well preserved after the chemical activation. For this purpose, we tested the N₂ adsorption/desorption isotherm of an MC-pristine-HK powder after evacuating the powder under vacuum at 25 °C for only 2 h. A TA-pristine-HK sample was also examined for comparison. The TA-pristine-HK sample was prepared by evacuating it under vacuum at a temperature of 150 °C for 12 h. With the isotherm results in hand, we determined Brunauer–Emmet–Teller (BET) specific surface areas of both MC-pristine-HK and TA-pristine-HK. Specifically, the BET areas were successfully obtained from the linear range of $0.0013 < P/P_0 < 0.0507$ for TA-pristine-HK and $0.0012 < P/P_0 < 0.0313$ for MC-pristine-HK, which pressure ranges were already identified by established “consistency criteria”.^{S5-S7} Eventually, we found that both samples yielded similar BET results, i.e., specific surface areas of approximately 1740 m²·g⁻¹ for TA-pristine-HK and approximately 1690 m²·g⁻¹ for MC-pristine-HK. These values are consistent within the (acceptable) error (see Figure S3). Additionally, the experimental values were in good agreement with values reported in the literature.^{S8-S11} This result indicates that MC treatment is a great method to activate the OCSs in HKUST-1 without structural damage.

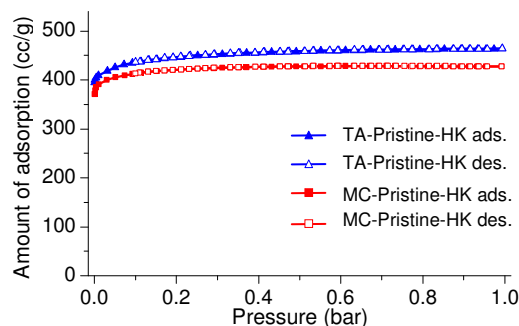


Figure S3. N₂ adsorption/desorption isotherms of TA-HK and MC-HK powders, as indicated.

Section S5. Raman Spectra of MC, EtOH, and H₂O Solvents

We wondered whether the Raman vibrational mode at approximately 289 cm⁻¹ in the sample of MC-HK (in MC) is a characteristic of the Cu-Cu paddle-wheel or MC. To determine the origin of the mode, we performed Raman analysis with bare MC solvent. The Raman spectrum in Figure S4 shows that the shift at approximately 289 cm⁻¹ is the characteristic of the scissoring vibration of Cl-C-Cl.^{S12} The spectrum also shows a stretching vibration mode at approximately 705 cm⁻¹, twist vibration mode of H-C-H at approximately 1150 cm⁻¹, and scissoring vibration mode of H-C-H at approximately 1415 cm⁻¹.

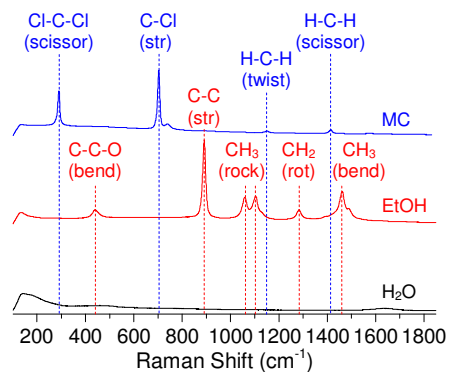


Figure S4. Raman spectra of MC, ethanol (EtOH), and water (H₂O), as indicated.

Section S6. Theoretical Studies for Raman Shift of Cu-Cu vibration in HKUST-1

To gain better understanding of the experimental results (see Figures 5a and 5b), we tried to simulate bond lengths and vibrational frequencies [$d_{\text{Cu-Cu-(X)}}$ and $\nu_{\text{Cu-Cu-(X)}}$, respectively; X = H₂O, MC (CH₂Cl₂), or OS (open-state: absence of coordinated molecule)] of H₂O-coordinated, MC-coordinated and open-state Cu-Cu in HKUST-1. The simulation was performed using density functional theory (DFT) with projector augmented wave (PAW) pseudopotentials,^{S13-S14} as implemented in the Vienna *ab initio* simulation package (VASP) code.^{S15} To incorporate an effect of exchange-correlation into the simulation, we employed the generalized gradient approximation (GGA) of PBE.^{S16} To simplify the simulation, we confined the space of a unit cell (for periodic model calculation) or a cluster (for cluster model calculation) only to a single k-point (the gamma point). Stretching vibrational frequencies of Cu-Cu bond were determined by calculating harmonic oscillation on the basis of the cluster-formation energy curves (Figure S5).^{S17}

Initially, we calculated bond length of open-state Cu-Cu bonding, $d_{\text{Cu-Cu-(OS)}}$, on the basis of periodic model in which whole 624 atoms within a unit cell of HKUST-1 are treated. The resulting $d_{\text{Cu-Cu-(OS)}}$ was 2.492 Å. We, however, could not succeed in obtaining stretching vibrational frequency of the Cu-Cu bond, $\nu_{\text{Cu-Cu-(OS)}}$, with this periodic model because the number of the atoms in the unit cell was too large to be treated in the simulation process.

Instead, we simulated it on the basis of an alternative model: cluster model in which the objective is finitely limited to a cluster consisting of a Cu-Cu paddle-wheel node and four BTC ligands (see inset of Figure S5 below). This cluster contains only 74 atoms—2 coppers, 24 oxygens, 36 carbons, and 12 hydrogens. This model could enable us to reduce time cost for the calculation and thereby, obtain reliable results. For instance, this model engendered $\nu_{\text{Cu-Cu-(OS)}}$ of 233 cm⁻¹. This value was quite close (or same) to the value (233 cm⁻¹) obtained from our Raman experiments (see Figure 5 and Table S1 below). Thus, we tentatively concluded that the cluster model can be suitably allowed for these simulations. In addition, this model resulted in a theoretical $d_{\text{Cu-Cu-(OS)}}$ value of 2.456 Å.

We wonder how the coordination of water molecule affects the bond length and vibrational frequency of Cu-Cu bond. With this question in mind, we firstly tested a simulation after placing two water molecules around axial open coordination sites (OCSs) of the paired Cu²⁺ centers in the modelled cluster. Consequently, the average $d_{\text{Cu-Cu-(H2O)}}$ was calculated to be 2.528 Å (see Table S1). This value indicates that the bond length is slightly elongated after water coordination (compare this 2.528 Å with the aforementioned $d_{\text{Cu-Cu-(OS)}}$ value of 2.456 Å). Regardless, a subsequently calculated bond length (2.216 Å) between Cu²⁺ and oxygen atom in H₂O molecule agreed with an experimental value (2.165 Å) previously reported in the literature.^{S18} This implies that this calculation method is highly reliable, and thus the simulated $d_{\text{Cu-Cu-(H2O)}}$ value itself and the elongation behavior after water coordination are acceptable. A further calculation for $\nu_{\text{Cu-Cu-(H2O)}}$ resulted in a frequency of 211 cm⁻¹. This value was somewhat higher related to the value obtained from our experiments (178 cm⁻¹). We ascribe this error to complicated vibration modes of the coordinated H₂O molecules. However, the red-shift from higher to lower frequencies after water coordination is an indisputable fact because the shift was commonly observed in both theory and experiment. (Remind the shifts from 233 to 211 cm⁻¹ in theoretical calculation and from 233 to 178 cm⁻¹ in experimental observation). We also tried to calculate vibration frequency of MC-coordinated Cu-Cu bond ($\nu_{\text{Cu-Cu-(MC)}}$), but could not obtain successful result due to the complexity of binding modes and vibrations of the coordinated MC molecule in calculations. Nevertheless, given that the aforementioned elongation of Cu-Cu bond and the red-shift of vibration frequency are highly dependent upon coordinating solvents and their coordination modes, we tentatively speculate that the vibrational frequency increases as the coordination strength of Lewis base (LB) molecules decreases. (We note that water molecule is a LB molecule that possesses lone-paired electrons in its oxygen.) We need more systematic studies for this

speculation. However, on the basis of the speculation and our experimental results, we also postulate that the coordination strength of MC ($\nu_{\text{Cu-Cu-(MC)}} = 219 \text{ cm}^{-1}$) is weaker than that of H_2O ($\nu_{\text{Cu-Cu-(H}_2\text{O)}} = 178 \text{ cm}^{-1}$), and thereby MC can be readily de-coordinated from the Cu^{2+} center with a low activation energy (thermal energy at room temperature).

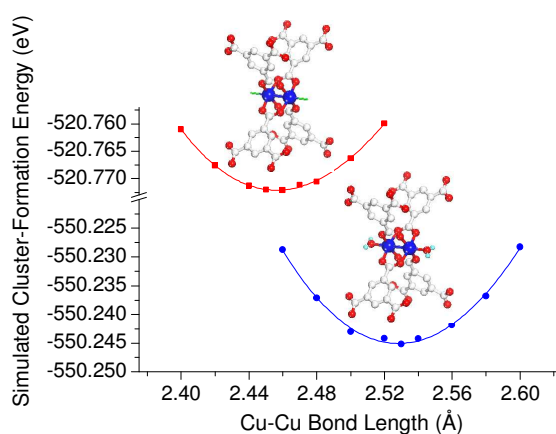
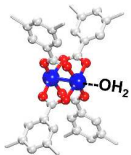

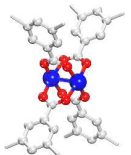


Figure S5. Plots of simulated stabilization energies of butterfly-shape cluster with respect to the Cu-Cu bond lengths. The modelled cluster of HKUST-1 was made consisting of a paddle-wheel-type Cu-Cu node and four BTC ligands. Both H_2O -coordinated and open-state Cu-Cu clusters were examined for the simulation, as indicated. Hydrogen atoms in BTCs were omitted for the sake of clarity.

Table S1. Bond Length ($d_{\text{Cu-Cu}}$) and Stretching Vibration Frequency ($\nu_{\text{Cu-Cu}}$) of Cu-Cu Bonding in HKUST-1

Physical parameters	Theory/Experiment	Coordination mode		
		H ₂ O-HKUST-1	MC-HKUST-1	Open-HKUST-1
				
Bond length $d_{\text{Cu-Cu}}$ (Å)	Periodic model	-	-	2.492
	Cluster model	2.528	-	2.456
	Experiments	2.628 ^{S18}	-	
Vibration frequencies $\nu_{\text{Cu-Cu}}$ (cm ⁻¹)	Cluster model	211	-	233
	Experiments	178	219	233

Section S7. Raman Spectra of Activated HKUST-1 after Exposure to Ambient Atmosphere

Figure 5d indicates that exposure of MC-HK to ambient atmosphere made the ligand-free Cu^{II} centers effectively re-coordinate with moist water molecules. At this point, we wondered whether the Raman shift of the stretching Cu-Cu vibration mode could eventually be recovered from a higher frequency (233 cm⁻¹) to a lower frequency (178 cm⁻¹) after longer exposure time to the ambient atmosphere. Obviously, we observed that the Raman peak shifted back to the lower frequency. We also found that a thermally activated HKUST-1 (TA-HK) sample exhibited the same behavior. Based on these results, we conclude that the Raman shift of the Cu-Cu vibration is reversible, depending upon the coordination fashion.

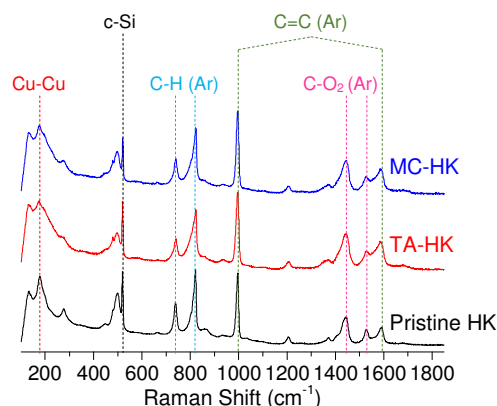


Figure S6. Raman spectra of pristine-HK, TA-HK, and MC-HK powder samples taken after exposure to ambient atmosphere for 2 h. We employed a crystalline silicon substrate for the powder sample in order to utilize the substrate as an internal standard.

Section S8. PXRD Patterns of Pristine and Activated Cu-MOF-2

To check whether the chemical activation of Cu-MOF-2 engenders behavior similar to TA, we monitored the changes in the PXRD patterns of pristine-, TA-, and MC-MOF-2. The PXRD patterns indicated that although the crystalline phase of the MOF-2 changed after activation, the superficial result of the chemical activation was the same as that of the TA (see Figure S7). Although more comprehensive studies are required to fully understand the phase transition behavior, this feature has often been observed.^{S4,S19-S21}

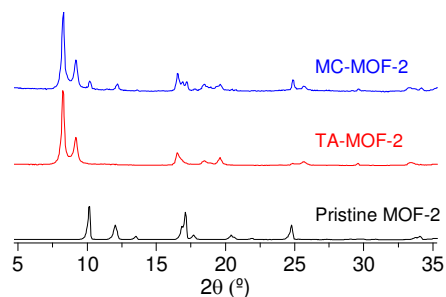


Figure S7. PXRD patterns of pristine-MOF-2, TA-MOF-2, and MC-MOF-2 powder samples, as indicated.

Section S9. ^1H -NMR, Raman, and BET Results for Room Temperature Evacuation of HKUST-1

To examine whether the open-metal site of Cu^{2+} ion can be activated at room temperature without MC treatment, we checked ^1H -NMR, Raman, and BET of a pristine HKUST-1 sample after applying only vacuum to the sample at room temperature for 2 h (without MC treatment). The ^1H -NMR and Raman spectra of the sample support that EtOH molecules bound to Cu^{2+} centers still remain as coordinated. BET result also demonstrates that applying only vacuum is not a good choice for activating HKUST-1 sample, showing its extremely low internal surface area (approximately $55\text{ m}^2\cdot\text{g}^{-1}$; compare this value with $1740\text{ m}^2\cdot\text{g}^{-1}$ for TA-pristine-HK and $1690\text{ m}^2\cdot\text{g}^{-1}$ for MC-pristine-HK described in Section S4). Also we note that, the acquisition time of measuring BET for the sample was too long to continue on the measurement (the acquisition time exceeded 90 hours, and the 90 h was a limit for the acquisition of the BET equipment that we used).

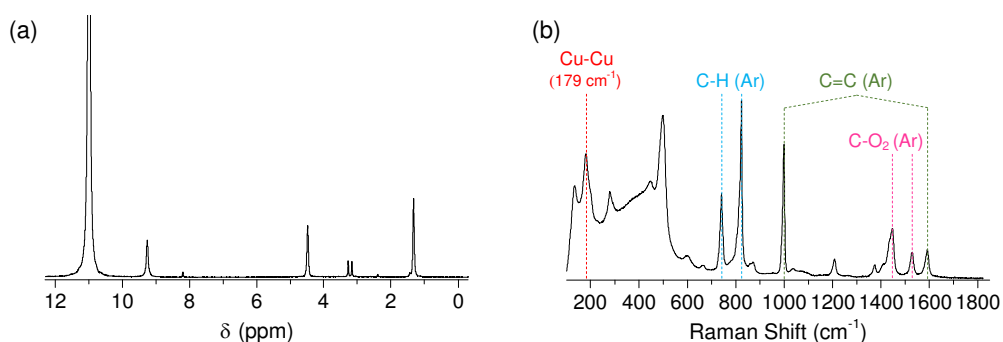


Figure S8. (a) ^1H -NMR and (b) Raman spectra of pristine-HK sample after applying only vacuum at room temperature for 2 h. The NMR spectrum was taken after completely dissolving the powder samples in D_2SO_4 .

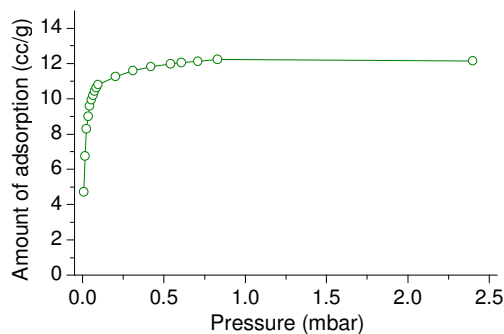


Figure S9. N_2 adsorption isotherms of a pristine-HK sample after applying only vacuum at room temperature for 2 h. We could not obtain a complete data set from BET due to the acquisition time limit of the equipment.

References

- S1. Jeong, N. C.; Samanta, B.; Lee, C. Y.; Farha, O. K.; Hupp, J. T. *J. Am. Chem. Soc.* **2012**, *134*, 51-54.
- S2. Mori, W.; Inoue, F.; Yoshida, K.; Nakayama, H.; Takamizawa, S.; Kishita, M. *Chem. Lett.* **1997**, *27*, 1219–1220.
- S3. Seki, K.; Takamizawa, S.; Mori, W. *Chem. Lett.* **2001**, *30*, 122–123.
- S4. Carson, C. G.; Hardcastle, K.; Schwartz, J.; Liu, X.; Hoffmann, C.; Gerhardt, R. A.; Tannenbaum, R. *Eur. J. Inorg. Chem.* **2009**, 2338–2343.
- S5. Rouquerol, J.; Llewellyn, P.; Rouquerol, F. *Stud. Surf. Sci. Catal.* **2007**, *160*, 49-56.
- S6. Walton, K.S.; Snurr, R.Q. *J. Am. Chem. Soc.* **2007**, *129*, 8552-8556.
- S7. Bae, Y.-S.; Yazaydin, A.O.; Snurr, R.Q. *Langmuir* **2010**, *26*, 5475-5483.
- S8. Panella, B.; Hirscher, M.; Pütter, H.; Müller, U. *Adv. Funct. Mater.* **2006**, *16*, 520-524.
- S9. Ma, S.; Zhou, H.-C. *Chem. Commun.* **2010**, *46*, 44-53.
- S10. Klimakow, M.; Klobes, P.; Thünemann, A. F.; Rademann, K.; Emmerling, F. *Chem. Mater.* **2010**, *22*, 5216-5221.
- S11. Song, X.; Jeong, S.; Kim, D.; Lah, M. S. *CrystEngComm.* **2012**, *14*, 5753-5756.
- S12. Shimanouchi, T. *Tables of Molecular Vibrational Frequencies Consolidated Volume I, National Bureau of Standards* **1972**, 1-160.
- S13. Blöchl, P. E. *Phys. Rev. B* **1994**, *50*, 17953-17979.
- S14. Kresse, G.; Joubert, D. *Phys. Rev. B* **1999**, *59*, 1758-1775.
- S15. Kresse, G.; Furthmüller, J. *Phys. Rev. B* **1996**, *54*, 11169-11186.
- S16. Perdew, J. P.; Burke, K.; Ernzerhof, M. *Phys. Rev. Lett.* **1996**, *77*, 3865-3868.
- S17. Van de Walle, C. G. *Phys. Rev. Lett.* **1998**, *80*, 2177-2180.
- S18. Chui, S. S.-Y.; Lo, S. M.-F.; Charmant, J. P. H.; Orpen, A. G.; Williams, I. D. *Science* **1999**, *283*, 1148-1150.
- S19. Tan, K.; Nijem, N.; Canepa, P.; Gong, Q.; Li, J.; Thonhauser, T.; Chabal, Y. J. *Chem. Mater.* **2012**, *24*, 3153-3167.
- S20. Chen, Z.; Xiang, S.; Zhao, D.; Chen, B. *Cryst. Growth Des.* **2009**, *9*, 5293-5296.
- S21. Prestipino, C.; Regli, L.; Vitillo, J. G.; Bonino, F.; Damin, A.; Lamberti, C.; Zecchina, A.; Solari, P. L.; Kongshaug, K. O.; Bordiga S. *Chem. Mater.* **2006**, *18*, 1337-1346.